A STUDY OF FROST ACCRETION ON THE THERMAL-HYDRAULIC PERFORMANCE OF FAN-SUPPLIED TUBE-FIN EVAPORATORS

Diogo L. da SILVA, diogo@polo.ufsc.br
Elias G. Colombo, elias@polo.ufsc.br
Giulia Baretta, giulia@polo.ufsc.br
Cláudio Melo, melo@polo.ufsc.br
Department of Mechanical Engineering, Federal University of Santa Catarina
88040970, Florianópolis-SC, Brazil, 55 48 3721 9397

Christian J. L. Hermes, chermes@ufpr.br
Department of Mechanical Engineering, Federal University of Paraná
PO Box 19011, 81531990, Curitiba-PR, Brazil, 55 41 3361 3239

Abstract. *Compact tube-fin evaporators have been extensively used in refrigeration cassetes for light commercial applications. Such refrigeration systems are space constrained and, therefore, the heat exchangers (condenser and evaporator) must have a large area-to-volume ratio. In addition, such applications require a subfreezing evaporating temperature that induces the growth of a frost layer on the finned surface, which in turn will eventually get blocked if a proper defrost strategy is not implemented. Before blocking the evaporator in full, the frost layer depletes the heat exchanger performance by increasing its thermal resistance and also by reducing the air flow rate supplied by the fan. Understanding how frost forms on these compact heat exchangers and how the fan is affected by the frost clogging is mandatory for designing robust refrigeration systems and also to devise efficient defrost strategies. Therefore, this study advances an experimental investigation on the frost accretion of tube-fin evaporators that accounted for the influence of the fan. Hence, fifteen experimental tests were carried out with four different evaporator coils (three with wavy fins and one with louvered fins) using a specially constructed wind-tunnel facility. It was found that the fan characteristics plays an important role on the evaporator thermal performance, indicating that under frosting conditions the fan-evaporator pair must be designed as a coupled system. Moreover, for the same operating conditions, the louvered fin evaporator showed to be more sensitive to the frost formation than the wavy fin samples.*

Keywords*: frost formation, tube-fin evaporator, fan-coil, thermo-hydraulic performance, experimental study*

1. INTRODUCTION

The efficient use of energy resources is a fundamental issue in modern society, not only due to its inherent environmental appeal but also to the steadily increasing costs, requiring changes in the way energy is generated, distributed and consumed. As the refrigeration is responsible for a large amount of the energy consumed worldwide, the Governments' energy policies have motivated the manufacturers to develop high efficiency refrigerators and also stimulated the consumers to purchase these products. However, the development of efficient refrigerators relies not only on the design of improved components (e.g., highly efficient compressors, anti-fouling condensers, and no-frost evaporators) but also on a proper matching between them.

In the light commercial refrigeration segment, the evaporator generally operates at temperatures below -10°C, leading to the formation of a frost layer on the evaporator surface. The frost accumulated on the evaporator coil decreases dramatically its performance due to the combined effect of the low thermal conductivity of the frost layer and an increase in air-side pressure drop, which reduces the air flow rate supplied by the fan. Such a double-effect was firstly observed by Stoecker (1957), who carried out an experimental study with regard to the effect of frost formation on the overall heat transfer coefficient and air-side pressure drop of industrial evaporators.

However, in spite of its importance, evaporator frosting research remained latent for many years until the 1990s, when Rite and Crawford (1991) conducted an experimental study on domestic finned-tube heat exchangers under frosting conditions and observed an increase in the air-side pressure drop and overall heat transfer coefficient, being the latter explained by an increase in the heat transfer surface and a decrease in the thermal contact resistance between fins and tubes. Later, Bejan *et al.* (1994) published a study of the performance of refrigeration systems operating under frosting conditions. The authors assumed a constant frost formation rate and identified an optimal on/off control strategy that minimizes the energy consumption of the whole system taking the electrical power used by the defrost heaters into account. However, the above mentioned studies did not account for the non-linear effect induced by the conflation between the frosted evaporator and the air-supply fan.

In a first attempt to fulfill this gap, Xia *et al.* (2006) studied the frosting, defrosting and re-frosting processes taking place on louvered-fin flat-tube heat exchangers and observed that the overall heat transfer coefficient decreases due to the reduction in air flow rate and also to the bridging of louver gaps. The authors concluded that the initial air pressure drop increases after each defrost cycle due to retention of condensed water droplets that eventually re-frost. Although such a study brought about important information on main factors affecting the frost formation phenomenon, a specific

investigation with regard to fan-supplied tube-fin evaporator with cooling capacities typical of light commercial refrigerators (~500 W) is still to be performed. This is, therefore, the main focus of this paper.

2. EXPERIMENTAL WORK

2.1 Experimental facility

The experimental apparatus is comprised of a rectangular cross-section wind-tunnel facility and a secondary-coolant refrigeration system. The former is used to control the air-side psychometric conditions at the evaporator inlet, whereas the latter sets the evaporator surface temperature. Figure 1 shows a schematic representation of the test rig, which is divided into two parts, the lower one, where the air is conditioned, and the upper one, where the test section is placed. At the lower part the air firstly flows through a 6.35 cm nozzle (1) used to measure the air flow rate according to the ASHRAE 51 (1999) standard, with a maximum uncertainty of ±0.003 m^3/s. The air is then cooled down by a coil (2), re-heated by an electric heater (3) and re-humidified by a water tray (4). All these processes are PID-controlled in order to guarantee the desired psychometric conditions at the inlet of the test section. The air flow rate is controlled by a computer-controlled variable-speed fan (5).

At the upper part of the test rig, the air temperature, relative humidity and pressure drop are measured up and downstream of the test section. The air temperature difference is measured by two grids of nine T-type thermocouples (TT) each, with a maximum uncertainty of ±0.2°C. The relative humidity difference is measured by two capacitive humidity transducers (HT) that provide a maximum uncertainty of ±1.5% (relative humidity). Furthermore, the air side pressure drop in the evaporator coil is measured by a differential pressure transducer (PT) with a maximum uncertainty of ±2.5 Pa. Finally, the frost formation rate and the heat transfer rate are determined indirectly through mass and energy balances, with uncertainties of ±0.1 kg/h and ±80 W, respectively.

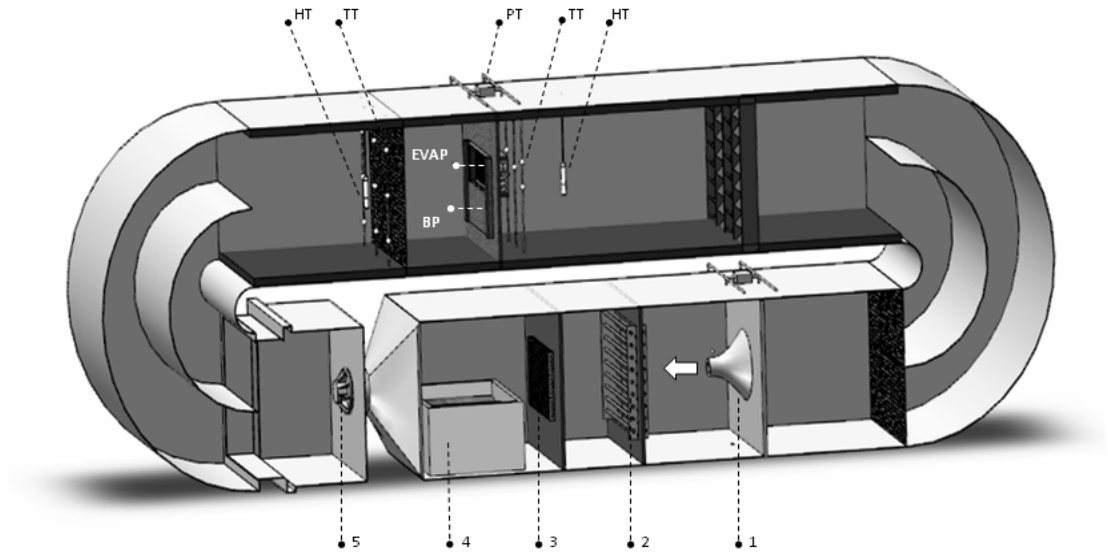

Figure 1. Schematic representation of the test rig

In the test section (upper part), the evaporator (EVAP) is fastened on a wooden structure comprised of a damper that directs the air flow either to the evaporator or to a passage located below the coil. Using such a device, the onset of the frost formation is started up just after the testing conditions have been properly reached. A chilled ethylene-glycol-water solution passes through to the coil to set the evaporator surface temperature, ensuring that the maximum temperature variation between the inlet and exit ports do not exceed 3.5°C.

The evaporator is a finned circular tube cross-flow heat exchanger, as showed in Fig. 2. The louvered and wavy fins are made of an aluminum alloy with a thickness of 0.2 mm. The tubes are made of cooper with an outer diameter of 10 mm and a wall thickness of 1 mm. The external dimensions of the front face, without including the return bends, are 320 x 152 mm, and the evaporator length in the air flow direction is 45 mm. The tubes are arranged into two columns with six tube rows each. The horizontal and vertical spacing between two adjacent tubes are 22 mm and 25 mm, respectively.

The air flow rate is controlled by a computer-driven variable-speed centrifugal fan that emulates the hydraulic behavior of any fan with capacities compatible with those used for light commercial refrigeration systems. The fan emulation procedure is carried out in an iterative way, converging when the difference between the actual and the air flow rate imposed to the facility (see Fig. 3) is smaller than a tolerance value not greater than 2%. Such a device permits

to analyze the frost formation on an evaporator coil using both constant and variable air flow rate in such a way as the decrease in the air flow caused by frost formation on evaporator can be took into account.

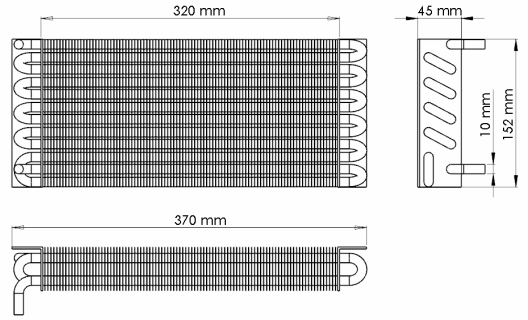

Figure 2. Schematic representation of the evaporator under testing

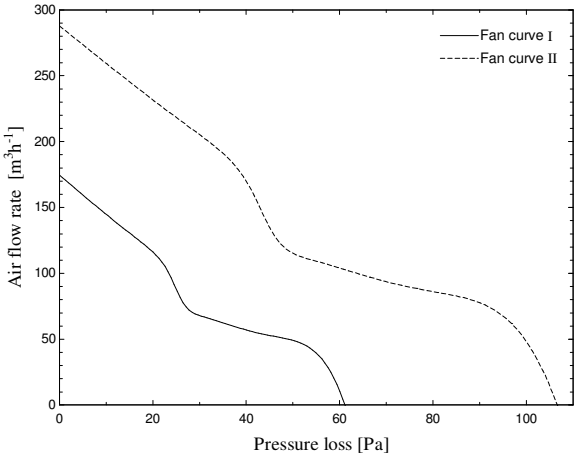

Figure 3. Characteristic curve of the fans emulated during the tests

2.2 Processing of raw data

Quasi-steady mass, energy and momentum balances over the evaporator were invoked in order to obtain the frost formation rate, the total heat transfer rate and air pressure drop, respectively, as follows:

$$m_f = m(\omega_1 - \omega_2) \tag{1}$$

$$q = mc_{p,a}(T_1 - T_2) + UA(T_{sur} - T_1) + m_f L \tag{2}$$

$$\Delta p = p_2 - p_1 \tag{3}$$

where m_f represents the frost formation rate [kg s^{-1}], m is the air flow rate [kg s^{-1}], ω is the humidity ratio [kg_s $kg^{-1}{}_a$], p is the air pressure [Pa], $c_{p,a}$ is the air specific heat at constant pressure [J kg^{-1} K^{-1}], T is the temperature [K], UA is an empirical correction coefficient [W K^{-1}] used to compensate the heat gain from the surroundings, L is the latent heat of dessublimation [J $kg^{-1}K^{-1}$] and q is the cooling capacity [W]. The mass of frost accumulated over time, M_f, is calculated from,

$$M_f = \int m_f \, dt \tag{4}$$

It is worthy of note that as the water-vapor transfer depends not only on the temperature differences but also on the latent heat transfer, so that the air enthalpies were used to calculate the overall heat transfer coefficient following the procedure described in Threlkeld *et al*. (1998),

$$U_h = \frac{q}{A_{wf}} \frac{\ln\left[(h_1 - h_{s,r2})/(h_2 - h_{s,r1})\right]}{(h_1 - h_{s,r2}) - (h_2 - h_{s,r1})} \tag{5}$$

where U_h is the overall heat transfer coefficient based on enthalpies differences [W m^{-2}J kg_a^{-1}], A_{wf} is the evaporator surface area without frost [m^2], h_1 and h_2 are the enthalpies of moist air [J kg_a^{-1}] evaluated at the evaporator inlet and exit positions, respectively, and $h_{s,r1}$ and $h_{s,r2}$ are the enthalpies of saturated moist air [J kg_a^{-1}] evaluated at refrigerant entering and leaving temperatures, respectively.

2.3 Test plan

The tests were planned to investigate how the number and type of fins, the air conditions, the evaporator surface temperature and the air flow rate affects the evaporator air pressure drop, the cooling capacity and the accumulated mass of frost. Supercooling degrees (*i.e.*, the temperature difference between the air-side dew-point at the evaporator inlet and the evaporator surface temperature, see Hermes *et al.*, 2009) of 3.5, 5.0, 10.0 and 14.5°C were used with different air flow rates and evaporator geometries (*i.e.*, different fin types and densities). Table 1 summarizes the test conditions, which covers the typical range of light commercial refrigeration applications. The experimental runs were conducted until the evaporator air flow rate or the total test time reached 60 m^3/h and 120 min, respectively.

Table 1. Summary of the experimental conditions

Test No.	Fin type	Fin density [fins/cm]	Supercooling [°C]	T_1 [°C]	ϕ_1 [%]	T_{evap} [°C]	Air flow rate [m³/h]
1	wavy	3.2	10.0	2.5	85	-10	150
2	wavy	3.2	14.5	7.0	85	-10	Fan curve I
3	wavy	3.2	10.0	2.5	85	-10	Fan curve I
4	wavy	3.2	5.0	2.5	85	-5	Fan curve I
5	wavy	3.2	3.5	2.5	74	-5	Fan curve I
6	wavy	4.7	14.5	7.0	85	-10	Fan curve I
7	wavy	4.7	10.0	2.5	85	-10	Fan curve I
8	wavy	4.7	5.0	2.5	85	-5	Fan curve I
9	wavy	4.7	3.5	2.5	74	-5	Fan curve I
10	wavy	2.2	14.5	7.0	85	-10	Fan curve I
11	wavy	2.2	10.0	2.5	85	-10	Fan curve I
12	wavy	2.2	14.5	7.0	85	-10	Fan curve II
13	wavy	2.2	10.0	2.5	85	-10	Fan curve II
14	louvered	2.2	14.5	7.0	85	-10	Fan curve I
15	louvered	2.2	10.0	2.5	85	-10	Fan curve I

3. RESULTS AND DISCUSSION

Figure 4 shows the time evolution of the frost accretion on the evaporator surface using the fan curve I. It can be seen that an increase in the fin density or in the supercooling degree causes the frost formation rate to increase. It is also observed a progressive reduction of the frost accumulation rate, which is more evident for tests with supercooling degrees of 10.0 and 14.5°C, due to a frost surface temperature reduction and also to a lower air flow rate supplied by the fan. Figure 5 shows a visual comparison between the initial and final states of fins subjected to a 35 min frost formation process, for an air flow rate of 150 m^3/h, an air temperature and relative humidity of 10°C and 50%, respectively, and an antifreeze solution inlet temperature of -10°C. The pictures show a significant reduction on the available free flow passage, which has remarkable influences upon the thermal-hydraulic performance of the evaporator. Also, it is important to emphasize that the supercooling degree was used in these analyzes as it condenses the information of four variables (p, T_a, ϕ and T_{evap}) into a single parameter.

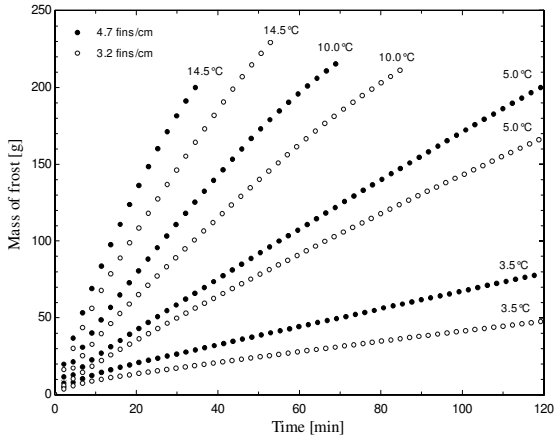

Figure 4. Accumulated mass of frost for different fin spacing and supercooling degrees

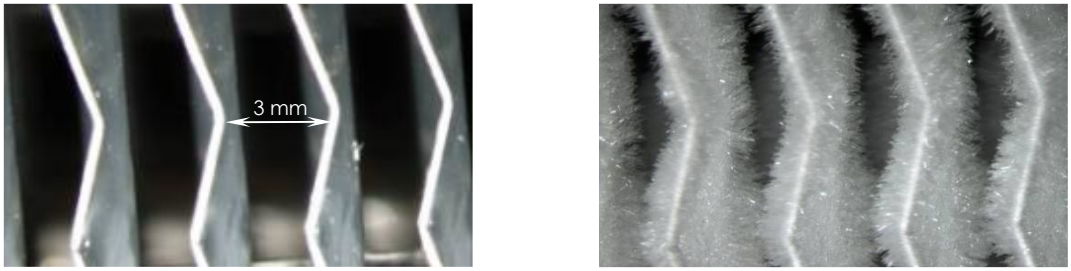

(a) (b)

Figure 5. Visualization of the fins surface before (a) and after (b) the frost formation process

Figure 6.a shows the influence of the accumulated mass of frost on the air-side pressure drop, where it can be noted that the supercooling degree and the number of fins increase the air pressure drop. It can be also observed that at low supercooling degrees (i.e., 3.5°C) the effect on the air pressure drop is negligible, indicating that a small amount of frost forms at such a condition, even with an evaporator surface temperature below 0°C (see Tab. 1). Figure 6.b illustrates how an increase in the air-side pressure drop affects the air flow rate, which decays dramatically for higher supercooling degrees (10.0 and 14.5°C). In these cases, the final air flow rate represents less than 50% of the initial value. On the other hand, an air flow rate reduction of 25% was observed for supercooling degrees ranging from 3.5 to 5.0°C. It can be also seen that a higher number of fins causes a larger reduction in the air flow rate for the same supercooling degree.

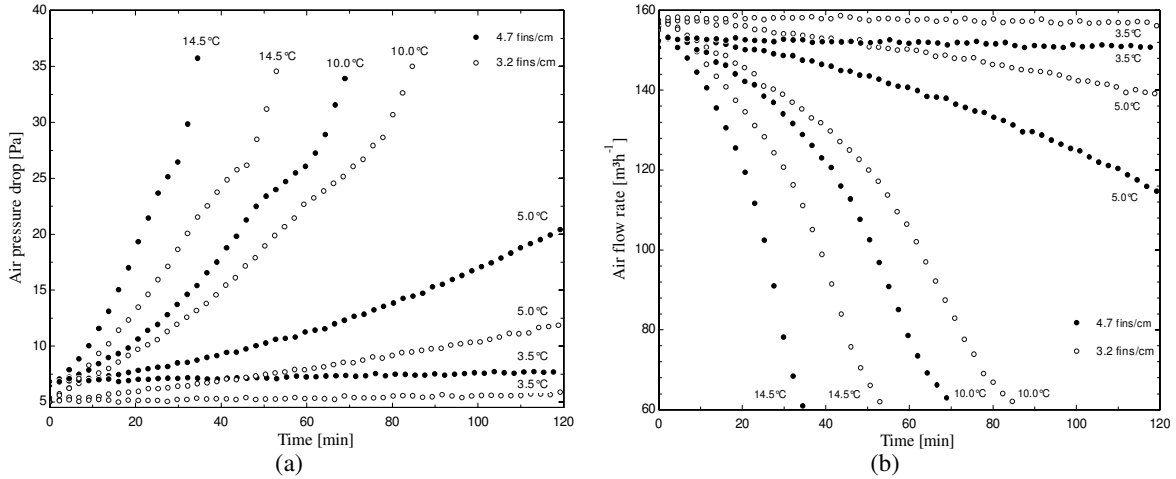

(a) (b)

Figure 6. Evaporator air-side pressure drop (a) and air flow rate (b) for different fin spacing and supercooling degrees

Figure 7.a shows the cooling capacity depletion caused by the frost formation process, considering the influence of the fan characteristics. For lower supercooling degrees (3.5 and 5.0°C) the high fin density heat exchanger seems to perform better. On the other hand, for higher supercooling degrees such a behavior is inverted. For instance, after 30 min, the high fin density evaporator, operating with a supercooling degree of 14.5°C, shows a 40% reduction on its cooling capacity, which is nearly the cooling capacity of a lower fin density evaporator operating under the same running condition. Figure 7.a also shows a comparison between the results of experiments where the air flow rate was held constant and varied according to the curve showed in Fig. 3. The analysis was carried out at the same operational conditions (see tests 1 and 3). For constant air flow rate it was observed a 15% cooling capacity reduction, whereas the tests with variable air flow rate show a 40% lower cooling capacity. These figures prove that the effect of the frost thermal insulation on the cooling capacity is not so important than the air flow rate reduction. The overall heat transfer coefficient as a function of time is plotted in Fig. 7.b, where it can be seen that the U_h-value experiences a significant reduction for higher supercooling degrees, which is due to a higher frost formation rate. Moreover, it can be observed in the tests with lower supercooling degrees that after experiencing an initial decrease, the U_h-value remains nearly constant over time.

In order to analyze the influence of the fan on the evaporator thermal-hydraulic performance, tests were carried out with the same evaporator (wavy fins, 2.2 fins/cm) for two supercooling degrees (10 and 14.5ºC) using the fan curves showed in Fig. 3 (see tests 10 to 13). Figure 8 shows that fan II induces a higher frost formation rate, resulting in an additional 50 g of frost at the end of the test. In spite of the additional mass of frost, Fig. 8.b shows that fan II is able to supply a higher air flow rate during the whole test, although the difference between the air flow rate supplied by fans I and II decreases with time as the fan II induces a higher reduction in the free flow passage than fan I. Figure 9 illustrates the time evolution of the cooling capacity (Fig. 9.a) and overall heat transfer coefficient (Fig. 9.b). For the same

supercooling degree, fan II showed a cooling capacity at least 20% higher than that provided by fan I. A similar behavior was found for the overall heat transfer coefficient.

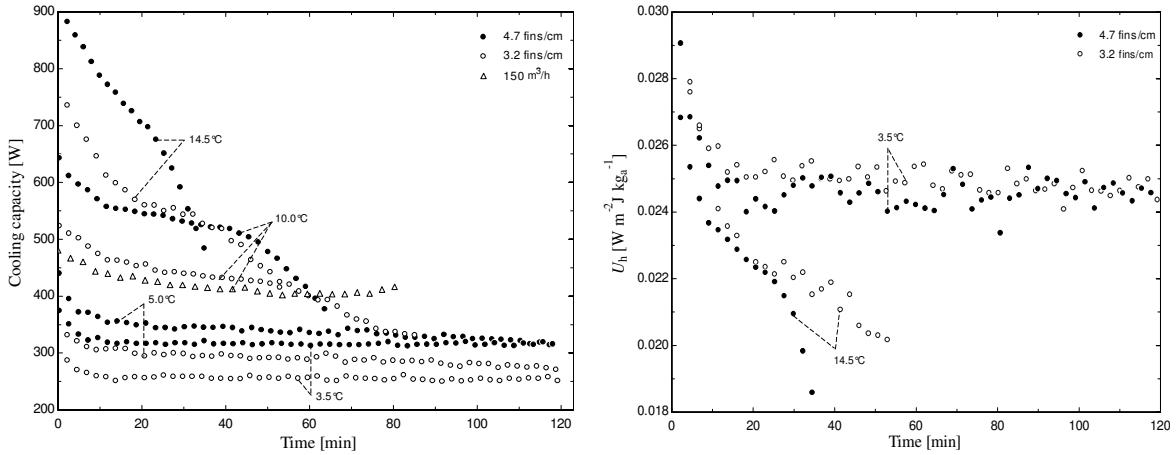

(a) (b)

Figure 7. Cooling capacity (a) and overall heat transfer coefficient (b) for different fin spacing and supercooling degrees

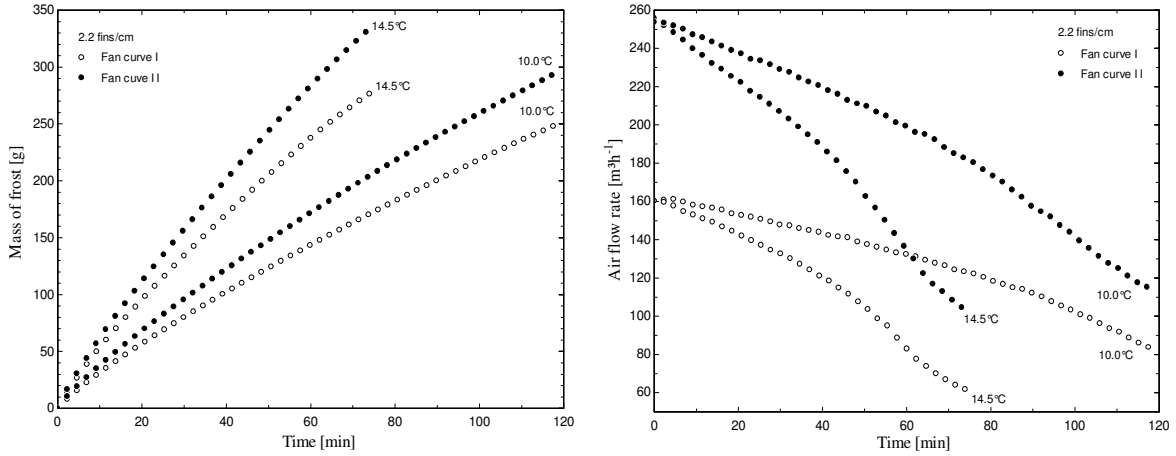

(a) (b)

Figure 8. Accumulated mass of frost (a) and air flow rate (b) for different fans and supercooling degrees

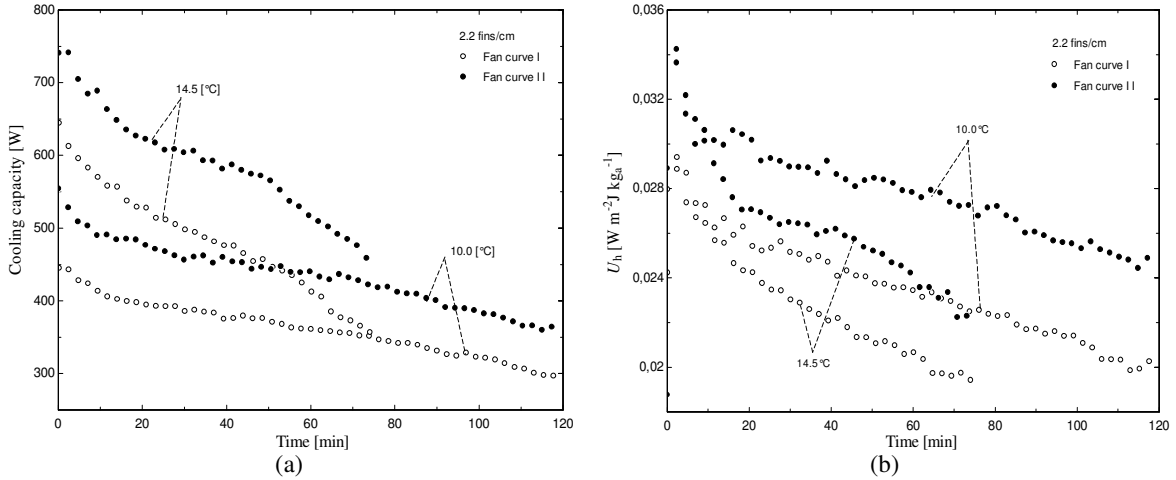

(a) (b)

Figure 9. Cooling capacity (a) and overall heat transfer coefficient (b) for different fans and supercooling degrees

The assessment of the effect of the type of fin (louvered or wavy) on the evaporator performance was carried out using two evaporators with 2.2 fins/cm operating under the very same frosting conditions (see tests 10, 11, 14 and 15).

Figure 10.a shows the mass of frost accumulated over time, where it can be noted that, for a same supercooling degree, both fin types provided similar results. However, as can be seen in Fig. 10.b, a the louvered-fin evaporator experiences a faster decrease on air flow rate due a higher restriction on free flow passage associated with the bridging of the louvered gaps.

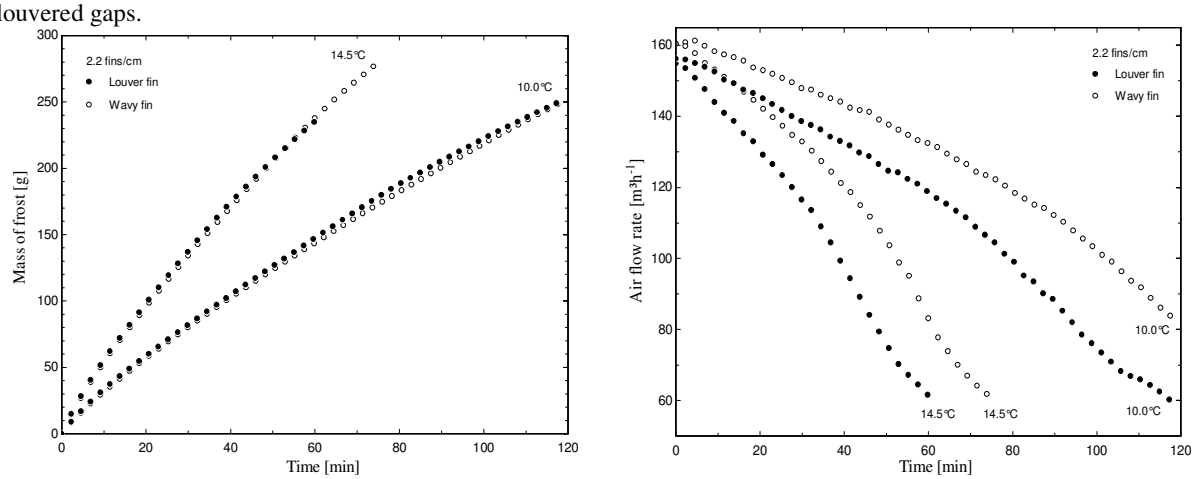

(a) (b)

Figure 10. Accumulated mass of frost (a) and air flow rate (b) for different fins and supercooling degrees

Furthermore, Fig. 11.a illustrates the time evolution of cooling capacity, where it can be observed that the louvered fins have a slightly better thermal performance in the beginning of the tests, where there was no significant frost formation on the finned-coil. Nonetheless, such a behavior is inverted after 40 and 60 minutes for supercooling degrees of 14.5 and 10.0°C, respectively, which is explained by the reduction of the fan-supplied air flow rate showed in Fig. 10.a. A similar conclusion can be extended to overall heat transfer coefficient (see Fig. 11.b), indicating that, under the very same frosting conditions, the use of louvered fins causes a higher depletion on the evaporator performance if compared to wavy-fin evaporators.

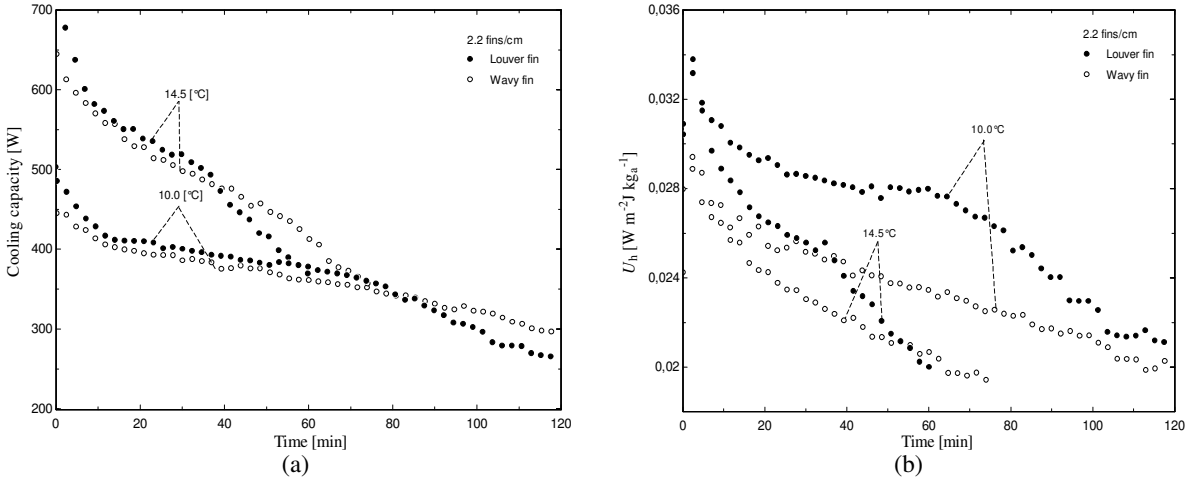

(a) (b)

Figure 11. Cooling capacity (a) and overall heat transfer coefficient (b) for different fins and supercooling degrees

4. CONCLUDING REMARKS

A purpose-built experimental facility was specially constructed for investigating the effect of frost formation on the thermo-hydraulic performance of tube-fin evaporator coils for refrigeration cassette applications. The facility is comprised of a wind-tunnel which controls and measures the air flow properties and also reproduces any fan characteristic curve used in light commercial appliances. The tests were carried out with two tube-fin heat exchangers operating under different evaporating temperatures and air psychometric conditions at the evaporator inlet. It was observed that the frost formation rate increases with the air flow rate, supercooling degree and the density of fins. A strict relation between accumulated mass of frost, air-side pressure drop and cooling capacity was also observed. Furthermore, the fan characteristic curve showed a great influence on the evaporator thermal performance, showing that a decrease in air flow rate is more important than the insulating effect of the frost layer.

The results also suggest that under frosting conditions the pair fan-evaporator must be designed as a coupled system, in order to maintain the original refrigeration capacity for longer periods, increasing the time between successive defrosting processes and, therefore, the thermal performance of the entire system. Finally, it was observed that under the same operating conditions, the louvered-fin evaporator showed a lower cooling capacity when compared to the wavy-fin evaporator. Such a behavior is due to a faster decrease in air flow rate associated with the additional pressure drop introduced by not only by the louvers but also by the frost bridges formed within the louver gaps.

5. ACKNOWLEDGEMENTS

This study was carried out at the POLO facilities under National Grant No. 573581/2008-8 (National Institute of Science and Technology in Refrigeration and Thermophysics) funded by the CNPq Agency. Financial support from Embraco S.A. is also duly acknowledged. The authors also gratefully thank Mr. Lucas Sassi, undergraduate student, for his valuable support with the experiments.

6. REFERENCES

ASHRAE Standard 51, 1999, Laboratory methods of testing fans for aerodynamic performance rating, American Society of Heating, Refrigeration and Air Conditioning Engineers, Atlanta, GA, USA

Bejan, A., Vargas, J.V.C., Lim, J.S., 1994, When to defrost a refrigerator, and when to remove the scale from the heat exchanger of a power plant, International Journal of Heat and Mass Transfer, Vol. 37 (3), pp. 523-532

Hermes, C.J.L., Piucco, R.O., Barbosa, Jr, J.R., Melo, C., 2009, A study of frost growth and densification on flat surfaces, Experimental Thermal and Fluid Science, Vol. 33, pp. 371-379

Rite, R.W., Crawford, R. R., 1991, The effect of frost accumulation on the performance of domestic refrigerator-freezer finned-tube evaporator coils, ASHRAE Transactions, Vol. 97(2), pp. 428-437

Stoecker, W.F., 1957, How frost formation on coils affects refrigeration systems, Refrigerating Engineering, Vol. 65, no. 2

Threlkeld, J.L., Kuehn, T.H., Ramsey, J.W., 1998, Thermal Environmental Engineering, 3rd ed., Prentice-Hall, USA

Xia, Y., Zhong Y., Hrnjak, P.S., Jacobi, A.M., 2006, Frost, defrost, and refrost and its impact on the air-side thermal-hydraulic performance of louvered-fin, flat-tube heat exchangers, Int. J. of Refrigeration, Vol. 29, pp. 1066-1079

7. NOMENCLATURE

Roman

A_{wf}	evaporator surface area without frost [m^2]
$c_{p,a}$	specific heat at constant pressure [J kg^{-1} K^{-1}]
h	air enthalpy [J/kg]
L	latent heat of dessublimation [J $kg^{-1}K^{-1}$]
m	air mass flow rate [kg s^{-1}]
m_f	frost formation rate [kg s^{-1}],
M_f	accumulated mass of frost [kg]
p	air pressure [Pa]
q	evaporator refrigeration capacity [W]
t	time [s]
T	temperature [°C]
U_h	heat transfer coefficient [W m^{-2} J^{-1} kg_a]
UA	empirical correction coefficient [W K^{-1}]

Greek

Δ	variation [-]
ϕ	relative humidity [%]
ω	humidity ratio [kg_s kg_a^{-1}]

Subscripts

a	dry air
evap	evaporator
f	frost
lat	latent
m	mean
s	steam
s,r	saturated at refrigerant temperature
sen	sensible
sur	surrounding
1	inlet
2	exit